Redox Biology 59 (2023) 102583

Contents lists available at ScienceDirect

Redox Biology

journal homepage: www.elsevier.com/locate/redox

Redox proteomics and structural analyses provide insightful implications for additional non-catalytic thiol-disulfide motifs in PDIs

Natalia Zamorano Cuervo [a], Nathalie Grandvaux [a,b,*]

[a] CRCHUM – Centre de Recherche du Centre Hospitalier de l'Université de Montréal, 900 rue Saint Denis, Montréal, H2X 0A9, Québec, Canada
[b] Department of Biochemistry and Molecular Medicine, Faculty of Medicine, Université de Montréal, Montréal, H3C 3J7, Québec, Canada

ARTICLE INFO

Keywords:
Protein disulfide isomerase
PDIA5
PDIA3
PDIA6
Cysteine
Redox
Oxidation
TRX-Like domain
Disulfide

ABSTRACT

Protein disulfide isomerases (PDIs) catalyze redox reactions that reduce, oxidize, or isomerize disulfide bonds and act as chaperones of proteins as they fold. The characteristic features of PDIs are the presence of one or more catalytic thioredoxin (TRX)-like domains harboring typical CXXC catalytic motifs responsible for redox reactions, as well as non-catalytic TRX-like domain. As increasing attention is paid to oxidative post-translational modifications of cysteines (Cys ox-PTMs) with the recognition that they control cellular signaling, strategies to identify sites of Cys ox-PTM by redox proteomics have been optimized. Exploration of an available Cys redoxome dataset supported by modeled structure provided arguments for the existence of an additional non-catalytic thiol-disulfide motif, distinct from those contained in the TRX type patterns, typical of PDIAs. Further structural analysis of PDIA3 and 6 allows us to consider the possibility that this hypothesis could be extended to other members of PDI. These elements invite future studies to decipher the exact role of these non-catalytic thiol-disulfide motifs in the functions of PDIs. Strategies that would allow to validate this hypothesis are discussed.

Changes of redox status take place during various cellular processes. While chronically elevated levels of reactive oxygen species (ROS) might be associated with oxidative damage, local changes in ROS levels act as redox switches regulating cellular signaling. ROS act as second messengers mainly through reversible oxidative post-translational modifications of cysteine residues (Cys ox-PTMs) that modulate protein structure, interaction with protein partners and ligand, localization, and activity [1–3]. The comprehension of the broad spectrum of ROS action has largely benefitted from the development of labeling techniques aimed at identifying proteins subjected to reversible Cys ox-PTMs [1,4]. This led to the discovery of new sites of reversible oxidation, but also to the validation of hypothetical redox dynamic processes, especially in highly reactive thiol-based enzymes such as thioredoxins, glutaredoxins, peroxiredoxins and protein disulfide isomerases (PDIs) [5–7].

1. Protein disulfide isomerases

PDIs are a large family of highly regulated redox proteins composed of 21 members [8]. PDIs are multifunctional thiol oxidoreductases that catalyze the oxidation, reduction, and isomerization of protein disulfide bonds, the most studied Cys ox-PTM [9]. Apart from peptide bonds, disulfides are the most prevalent covalent link between two amino acids and are one of the most frequent PTMs [10–12]. Disulfide bonds play important roles in protein structure and function, but also in the folding of nascent peptides in the ER [13,14]. Members of the PDI family are involved in the pathology of several diseases associated with changes in ROS levels, including cardiovascular diseases and cancer [15–18]. In cancer, increased expression of PDIs is also thought to confer resistance against chemotherapy-induced apoptosis [17]. These observations have led to numerous studies aiming at evaluating PDIs inhibitors as therapeutic strategies [15,18–20]. Human PDIs also play important roles in virus infections [8]. For instance, Influenza A virus (IAV) uses PDIA3 for the proper folding of its surface hemagglutinin (HA) glycoprotein [21]. PDIs are also implicated in the folding of the pre-membrane (pre-M) protein and envelope (E) glycoproteins of Dengue virus [22] and PDIA1 regulates human immunodeficiency virus (HIV) entry through interaction with the envelope glycoprotein gp120 [23]. Given the involvement of PDIs in many pathophysiological processes, their function, and the mechanisms by which they regulate the redox status of Cys in target proteins have been extensively explored.

PDIs are characterized by at least one TRX-like domain [9] which is either catalytically active (a or a') or non-catalytic (b or b'). Position and

* Corresponding author. CRCHUM – Centre de Recherche du Centre Hospitalier de l'Université de Montréal, 900 rue Saint Denis, Montréal, H2X 0A9, Québec, Canada.
E-mail address: nathalie.grandvaux@umontreal.ca (N. Grandvaux).

https://doi.org/10.1016/j.redox.2022.102583
Received 23 October 2022; Received in revised form 12 November 2022; Accepted 19 December 2022
Available online 20 December 2022

catalytic functions of the TRX-like domains vary amongst PDIs ensuring distinct redox properties and substrates specificities. The typical active site of the catalytic TRX-like domain is a CXXC motif that is involved in the reduction, oxidation, or isomerization of disulfide bonds within misfolded proteins [24]. Although considered not redox active, b and b' non-catalytic TRX-like domains, for which a consensus motif has not yet been proposed, are essential for the activity of PDIs because they mediate specific substrate recognition and binding [25–29], chaperon functions [30–32] and structure stabilization to favor interactions between the catalytic domain and the substrate [9,30,33,34].

Amongst PDIs, the closely related PDIA1-6 members possess at least two a-type catalytic TRX-like domains and at least one b-type non catalytic TRX-like domain [25]. In addition, PDIAs present an ER targeting signal sequence in the C terminal region (Cter) [25] (Fig. 1A and B). PDIA1, 2 and 3 exhibit a typical organization with two catalytic TRX-like domains located in the N-terminal (Nter) and Cter regions separated by two non-catalytic TRX-like domains (Fig. 1A). PDIA4 has a similar organization, but has three catalytic domains, two of which are located in the Nter [35]. PDIA6 possesses two catalytic domains located side by side in the Nter region [35], but mainly differs from the typical organization by the absence of a second non-catalytic domain. PDIA5 is unique in that it also possesses only one characterized non-catalytic TRX-like domain positioned at the Nter end followed by 3 side-by-side catalytic domains [35,36].

2. Protein disulfide isomerase A5

Knowledge about PDIA5 is still scarce. PDIA5, also known as Protein disulfide isomerase-related protein (PDIR) [37], was firstly identified in 1995 and classified as a member of the PDI family based on the presence of three catalytic a-type TRX-like domains (aa 134–261; aa 270–384; aa 385–506) containing CXXC catalytic sites ($C^{182}SMC^{185}$, $C^{305}GHC^{308}$ and $C^{426}PHC^{429}$) (Fig. 1A) [37]. PDIA5 also possesses one non-catalytic b-type TRX-like domain (aa 29–150). It is the only PDIA5 domain for which a crystal structure is available. Three Cys (Cys^{81}, Cys^{85} and Cys^{94}) are present in this domain. The structure shows a disulfide bond between Cys^{85} and Cys^{94}, while Cys^{81} remains free [36]. Sequence alignment showed evolutionary conservation of Cys^{85} and Cys^{94}, but not Cys^{81}. The lack of conservation of the latter amongst PDIA5s orthologs supports the idea that it is not involved in redox reactions [36]. The crystal structure also shows a positively charged surface rich in Lysine. As non-catalytic TRX-like domains are involved in the binding of PDI substrates, it is believed that PDIA5 interactors must possess a negatively charged surface, as observed in calreticulin [36,38]. Several PDIA5 substrates have being identified over the years, including α1-antitrypsin [39], Neudesin (NENF) [40,41], Protein phosphatase inhibitor 2 (PPP1R2) [42], DNA-directed RNA polymerase II subunit RPB7 (POLR2G) [43], Pleiotropic regulator 1 (PLRG1) [43] and Cell division cycle 5-like protein (CDC5L) [42]. Whether they exhibit a negatively charged surface at the interface with PDIA5 remains to be determined.

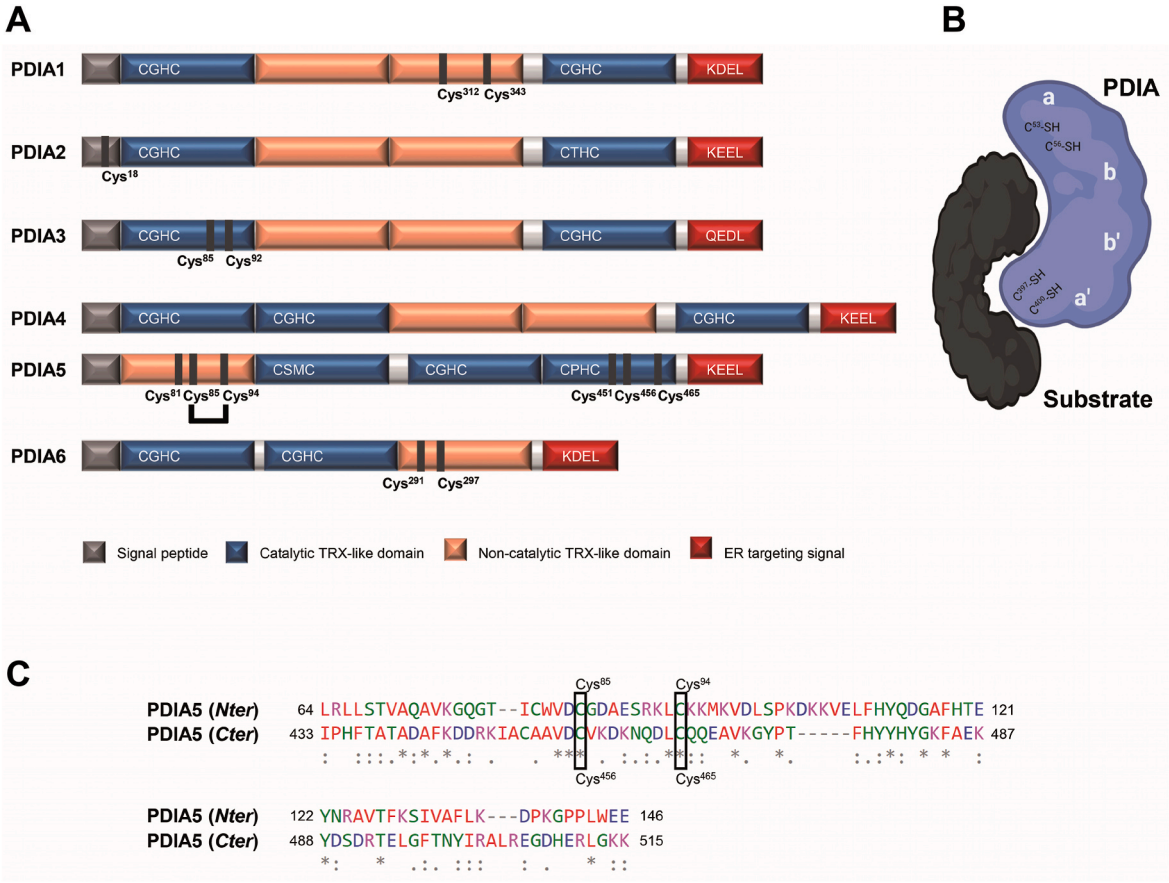

Fig. 1. Linear sequences of PDIA1 to 6. Catalytic TRX-like domains are shown in blue and the CXXC motif is depicted inside the blocks. Non-catalytic TRX-like domains are shown in orange, ER signal sequence appears in red and signal peptides are in dark gray. Position of Cys residues discussed in this paper are outlined. For PDIA5, a disulfide bond is depicted between two Cys. **B.** Schematic of a classical PDI (here PDIA1, in blue) bound to its substrate (in black) during an ongoing disulfide exchange. Position of catalytic (a and a') and non-catalytic (b and b') TRX-like domains are indicated. **C.** Sequence alignment of the Nter region of PDIA5 (aa 64–146) versus the Cter region of the protein (aa 433–515). (For interpretation of the references to colour in this figure legend, the reader is referred to the Web version of this article.)

Of note, three Cys residues (Cys^{451}, Cys^{456} and Cys^{465}) are present in the Cter region of the third catalytic TRX-like domain outside of the known CXXC catalytic motif (Fig. 1A). We noticed a partial alignment of these amino acids with those of the non-catalytic b domain, namely an alignment of Cys^{85} and Cys^{94} with Cys^{456} and Cys^{465}, respectively (Fig. 1C). Although there is no report yet of a role or redox activity of these C-terminal Cys of PDIA5, redox active Cys outside of the catalytic motifs have been reported for PDIA1. In this case, Cys^{312} and Cys^{343} located in the b' non-catalytic domain are subjected to nitrosylation [44]. Cys^{343} nitrosylation appears to be stable and negatively impacts the activity of the catalytic motif located further in the structure [45]. Additionally, Cys^{18} in PDIA2 located in the Nter ER signal peptide forms intermolecular disulfide bonds with another subunit of PDIA2 allowing the formation of oligomers with increased chaperone activity. Disulfide bonds were found to be reversible depending on the oxidative or reducing conditions and were therefore considered redox active [46]. Regarding PDIA3 and PDIA6, there is so far no information on the existence of active redox Cys, other than those in the catalytic motifs. However, some Cys of PDIA3 and PDIA6 are organized into CXXXXXXC (CX_6C) or CXXXXXC (CX_5C) motifs and could potentially be involved in redox processes [47–50].

3. Redox proteomics and structural insights highlight a possible role of previously unrecognized redox active Cys in the Cter extremity of PDIA5

In a previous study, we performed a proteome wide identification of Cys ox-PTMs in U937 cells at basal levels and following exposure to hypochlorous acid (HOCl) or diamide. Our approach was based on a workflow allowing labeling of reversibly modified Cys independently of the type of oxidation using a maleimide (Mal)-(Polyethylene glycol)$_2$-Biotin (Mal-PEG_2-Bio)-based bioswitch coupled to mass spectrometry (LC-MS/MS) [51]. In this workflow (Fig. 2A), reduced Cys are labeled with NEM, while oxidized Cys carry a Mal-PEG-Bio moiety. The publicly available proteomics datasets from this previous study (ProteomeXchange, identifier PXD020270) were re-analyzed to extract information regarding the redox modifications of PDIA5 Cys residues. All MS/MS data were analyzed using Mascot (Matrix Science, London, UK; version 2.4.0). Mascot was set up to search against an integrated proteome database, containing 99739 entries extracted from NCBI, assuming the digestion enzyme trypsin at a maximum of 1 missed cleavage. Tolerance of 0.60 Da was accepted for the fragment ion mass during the Mascot search, with a parent ion tolerance of 10.0 PPM. Variable modifications specified in the Mascot search were Methionine oxidation (Met+15.99Da), Cys alkylation with NEM (Cys+125.05Da) and Mal-PEG_2-Bio-labeled Cys (Cys+525.23Da) (Fig. 2A). Scaffold (version Scaffold 4.8.4, Proteome Software Inc., Portland, OR) was used to validate MS/MS based peptide and protein identification. Only peptides containing at least 1 Cys-ox-PTMs and detected in at least two out of the three biological replicates were considered for spectral counting. Standard cut-offs of significance for peptide ion signal peak intensity were calculated via Scaffold algorithms [52,53]. Identification of peptides was accepted if it could be established at greater than 95.0% probability by the Peptide Prophet algorithm [54] with a false discovery rate (FDR) $< 1\%$ and Scaffold delta-mass correction. Identification of proteins was accepted if it could be established at greater than 95.0% probability and contained at least 1 identified oxidized peptide. The Protein Prophet algorithm was used to assign protein probabilities [55].

Several PDIA5 peptides encompassing two Cys modified with different labels, i.e., NEM or Mal-PEG_2-Bio, reflecting distinct redox status were found (Fig. 2A–C). A first peptide encompassed Cys^{81} and Cys^{85} contained in the non-catalytic b domain. While Cys^{81} was labeled with NEM, Cys^{85} was modified by Mal-PEG_2-Bio both at basal levels and after oxidant exposure, indicating reduced status and reversible oxidation under both conditions, respectively. The detection of reduced Cys^{81} and oxidized Cys^{85} are in agreement with the crystal structure of the Nter inactive region, which shows a disulfide bond between Cys^{85} and Cys^{94}, but no disulfide involving Cys^{81} [36]. Intrinsic limitations of our workflow lie in the sensitivity and in the fact that only peptides containing at least one oxidized Cys labeled with Mal-PEG-Bio are pull down. We did not detect peptide containing Cys^{94} and therefore we could not accurately determine the oxidation state of Cys^{94}. While it is possible that Cys^{94} was in a reduced state in both conditions and contained in a peptide without oxidized Cys, it would be inconsistent with the crystal structure and models suggesting engagement of Cys^{94} in a disulfide bond with Cys^{85} in the non-catalytic domain of PDIA5. Rather, our observation that the redox status of Cys^{85} remains unchanged upon oxidant exposure, likely engaged in a disulfide bond with Cys^{94}, is consistent with the idea that the Nter region of PDIA5 is a non-catalytic TRX-like domain.

Our MS data also informed about the redox states of Cys in the Cter of PDIA5, which has yet to be structurally and functionally defined. At basal levels, Cys^{451} was reduced, while Cys^{456} in the same peptide was oxidized. Cys^{465}, identified on a different peptide, carried a Mal-PEG_2-Bio moiety, indicative of a reversible oxidation (Fig. 2B). Upon exposure to oxidants, the peptide encompassing Cys^{451} and Cys^{456} was no longer detected, suggesting that it could not be pulled down because both thiols were in a reduced form. However, we cannot exclude that these residues were subjected to irreversible oxidation that are not detectable by the bioswitch method used in our study. In contrast, Cys^{465} remained oxidized (Fig. 2C). In any case, this observation is indicative of a redox dynamic involving Cys at the Cter of PDIA5 in response to oxidants.

Out of the 519 amino acids of PDIA5, the only available crystallographic structure corresponds to the region encompassing amino acids 29–150 that is contained in the non-catalytic TRX-like domain [36]. In the absence of the complete crystallographic structure, we used the recent modeling of the full-length PDIA5 proposed by Alphafold (PDB AF-Q14554-F1) [56,57]. The template was visualized with PyMOL. Consistent with the crystal structure, a disulfide bond is observed in the Nter non-catalytic TRX-like domain between Cys^{85} and Cys^{94}, but not Cys^{81} [36] (Fig. 2D). In the Cter, a disulfide bond is predicted between Cys^{456} and Cys^{465}, but none involving Cys^{451}. This disulfide bond could explain the oxidized state of Cys^{456} and Cys^{465} at basal level observed by proteomics. Next, we used the PyTMs plugin to introduce sulfenylation [58] in silico to mimic Cys oxidative modification observed by MS after oxidant exposure. For this, we did not change the redox status of Cys^{81}, Cys^{85} and Cys^{94}, hence the presence of the disulfide bond (Fig. 2E). In the Cter region, Cys^{451} was left reduced. We reduced Cys^{456} and added a sulfenyl group on Cys^{465}, thereby causing the disruption of the disulfide bond. Prediction of steric structural strains [vdW clashes, [58]] with the PyTMs plugin shows clashes distributed throughout the structure, including one localized very close to the sulfenylated Cys^{465}. This suggests that PDIA5 in this redox status must undergo a change in conformation to adopt a stable structure.

With this in mind, two plausible scenarios can be considered. A first option could be that the Cys^{456}-Cys^{465} disulfide bond observed in the inactivated state is disrupted upon activation by oxidant exposure so that a disulfide bond can be formed between Cys^{465} and PDIA5 interacting regulator or substrate. The latter would be possible for highly complex client for which classical interaction with catalytic Cys is not sufficient. In this scenario, Cys^{456} would then be reduced. Similar to the role of the non-catalytic Trx-like domain, the conformational change induced by the disulfide bond transfer could serve to bring the catalytic domain of PDIA5 closer to the substrate to allow the redox reaction [9,34]. A second possible scenario would be that the disruption of the disulfide bond and the subsequent conformational change exposes the contact surfaces necessary for the interaction of a redox substrate. In this case, the disulfide bond would be considered allosteric and the redox dynamics would affect substrate recognition and therefore PDI activity [30]. Finally, an alternative possibility would be that the conformational change induced by the redox dynamics would instead expose Cys^{451} or Cys^{456} thus making them accessible for interaction with a substrate or to

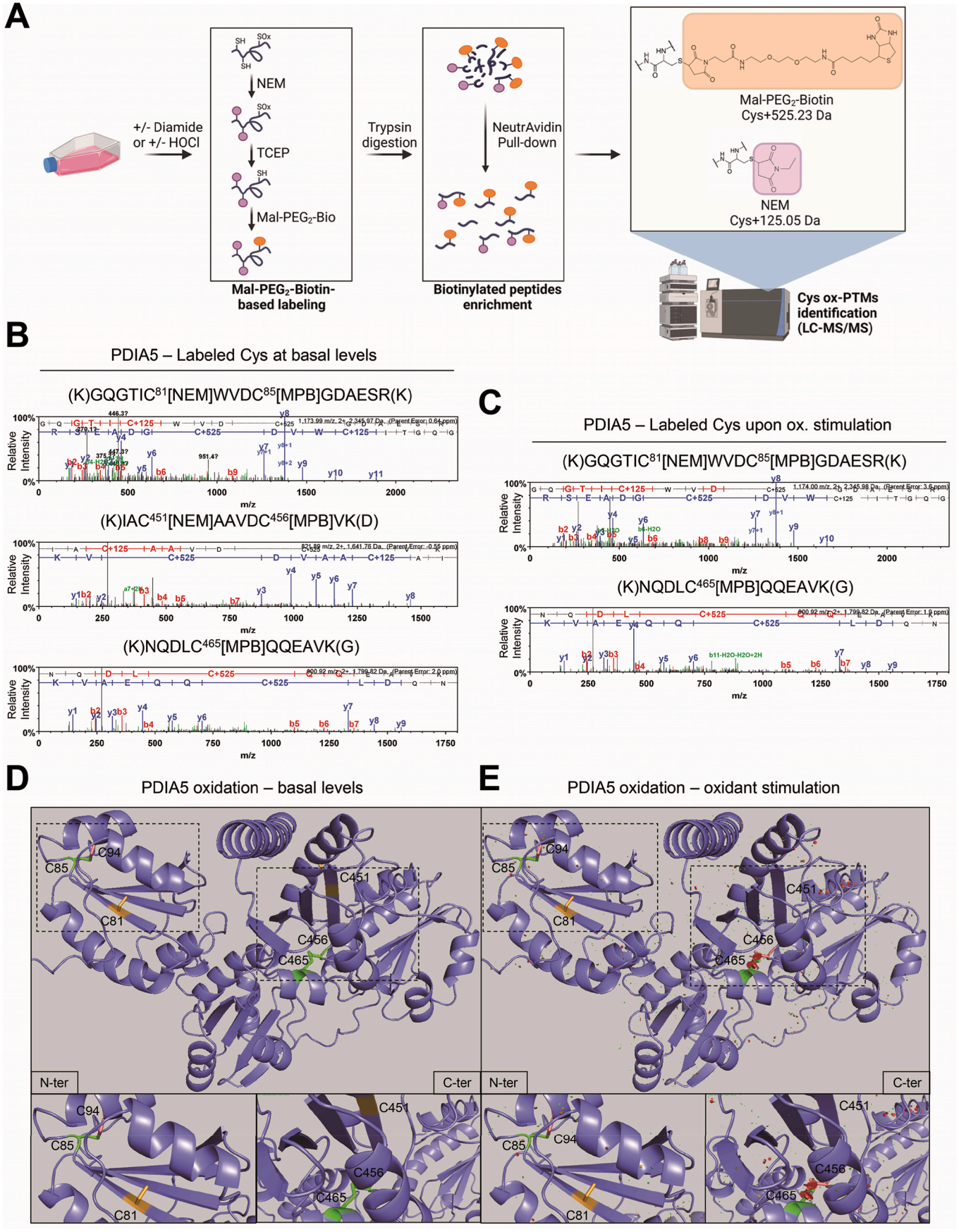

(caption on next page)

Fig. 2. Oxidation of protein disulfide isomerase 5 (PDIA5) at basal levels and upon oxidant exposure and impact on the structure. A. Schematic of the workflow followed in Ref. [51] to label reduced and reversible oxidized Cys. Briefly, Cys in whole cell extracts from unstimulated U937 cells, or cells exposed to oxidants (diamide or HOCl) were subjected to alkylation (NEM) and Mal-PEG_2-Biotin based labeling. Proteins were digested with trypsin and the fraction of Mal-PEG_2-Bio-labeled peptides was enriched by a NeutrAvidin pull-down. Samples were analyzed by LC-MS/MS to identify peptides containing Mal-PEG_2-Bio-labeled Cys sites (Cys+525.23 Da) and NEM-labeled Cys sites (Cys+125.05 Da). N-ethylmaleimide (NEM), tris(2-carboxyethyl)phosphine (TCEP), Maleimide-(Polyethylene Glycol)2-Biotin (Mal-PEG_2-Bio). **B–C.** Fragment spectra of PDIA5 peptides containing Mal-PEG_2-Bio- (MPB, C+525) and NEM (C+125) Cys at basal levels (**B**) and upon diamide/HOCl exposure (**C**). The fragment peaks of both b and y ions are shown in the spectra in red and blue, respectively. **D-E.** Modeled structure of the full-length PDIA5 proposed by Alphafold (PDB AF-Q14554-F1) [56,57]. Reduced Cys are represented in orange, oxidized Cys are in green. Cys that were not identified in our results but are important for the structural analysis are shown in salmon. At basal levels (**D**), in the N-terminal (N-ter) of the protein, Cys^{81} is reduced, while Cys^{85} forms a disulfide bond with Cys^{94}. In the C-terminal (C-ter), Cys^{456} and Cys^{465} also form a disulfide bond, but Cys^{451} appears reduced. Upon oxidant exposure (**E**), the redox states of Cys^{81} and Cys^{85} do not differ from those observed at basal levels. In the C-ter only Cys^{465} remains oxidized. Van der Waals (vdW) clashes due to the oxidation of Cys^{465} appear in red. (For interpretation of the references to colour in this figure legend, the reader is referred to the Web version of this article.)

carry out redox functions.

Taken together, MS data documenting changes in redox states of Cys in Cter supported by information from the modeled structure of full-length PDIA5 lead us to propose that there is a previously unrecognized non-classical redox dynamic region. at the Cter end of PDIA5. This invites further studies to characterize the role of this region in PDIA5 activity. Additionally, it warranted re-analysis of sequences from other PDIAs to determine if a similar region can be identified.

4. Prediction of disulfide bond dynamics in PDIA3 and PDIA6 between Cys outside catalytic motifs provides insight into potential impact on structure and function

The observation that PDIA3 and PDIA6 possess Cys located in CX_6C

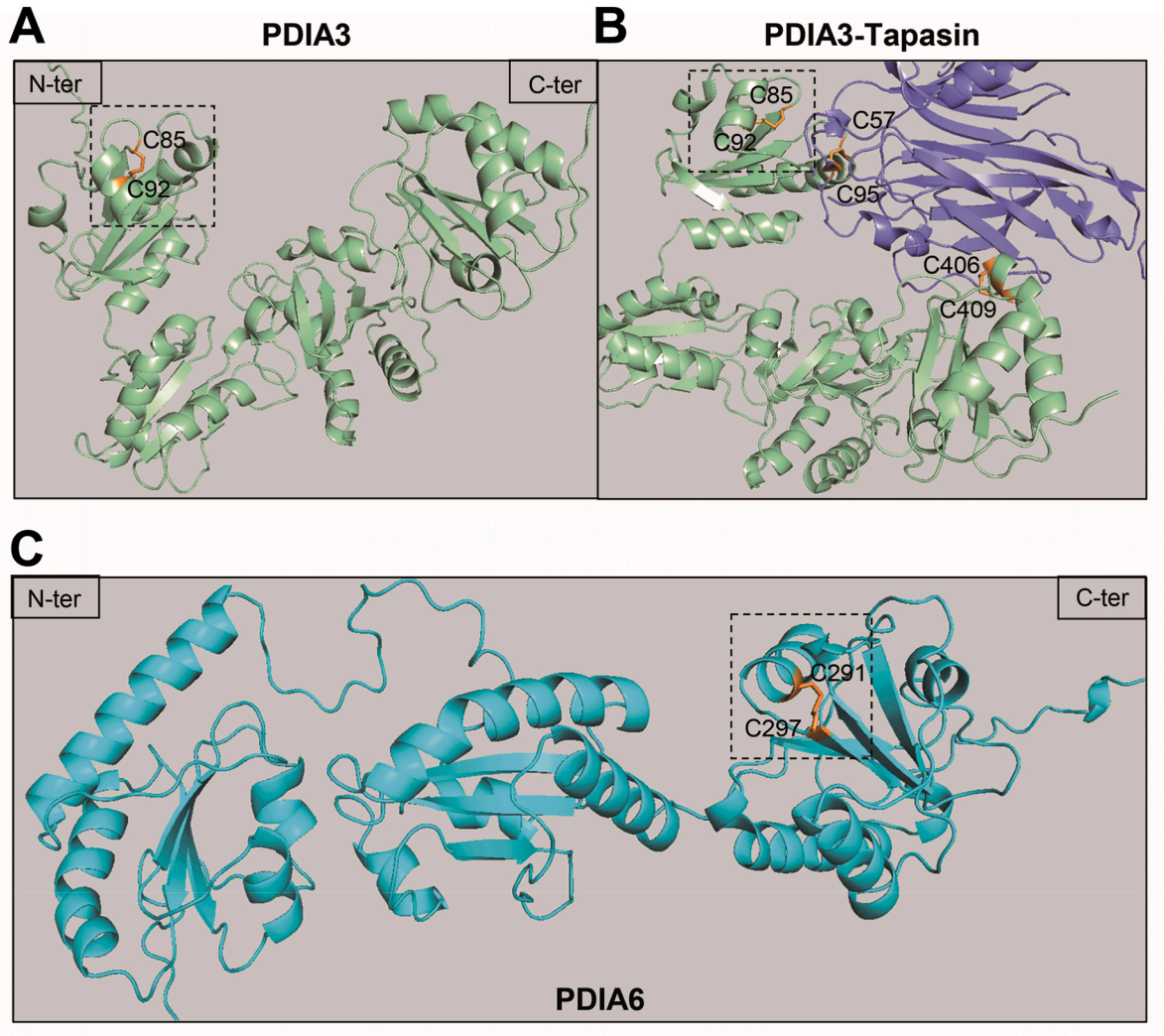

Fig. 3. Presence of disulfide bonds apart from known redox active motifs in modeled structures of PDIA3 and PDIA6. A. Modeled structure of the full-length PDIA3 (PDB AF-P30101-F1) proposed by Alphafold [56,57]. Cys^{85} and Cys^{92} involved in disulfide bonds are represented in orange, with the bonds as sticks. **B.** Structure of PDIA3 interacting with Tapasin (PBD 6ENY). PDIA3 is represented in green, Tapasin in blue, Cys involved in disulfide bonds are in orange (Cys^{85}-Cys^{92}, Cys^{406}-Cys^{409} and PDIA3 Cys^{57}-Tapasin Cys^{95}). Disulfide bonds appear as sticks. **C.** Modeled structure of the full-length PDIA6 (PDB AF-Q15084-F1) proposed by Alphafold, in cyan. Cys^{291} and Cys^{297} involved in disulfide bonds are represented in orange, with the bonds as sticks. (For interpretation of the references to colour in this figure legend, the reader is referred to the Web version of this article.)

or CX_5C motifs, respectively, prompted us to evaluate the structures to inform on their potential role. As available structures obtained either by X-ray diffraction or nuclear magnetic resonance (NMR) do not encompass the complete protein, we visualized the recently modeled full-length structures proposed by Alphafold (PDB AF-P30101-F1 and AF-Q15084-F1, respectively) [56,57] using PyMOL. In the case of PDIA3, a disulfide bond is predicted between Cys^{85} and Cys^{92} located in the CTANTNTC motif in the Nter a-type domain (aa 25–133, Fig. 3A), but distinct from the catalytic motif ($C^{57}GHC^{60}$). In PDIA6, a disulfide bond is predicted between Cys^{291} and Cys^{297} that belong to the CEEHQLC motif located toward the Cter region, within the non-catalytic TRX-like domain (aa 288–436, Fig. 3C). While none of the available PDIA6 3D structures allows the visualization of Cys^{291} and Cys^{297}, there is an almost complete X-ray diffraction structure for PDIA3 interacting with Tapasin. This structure confirmed the presence of a disulfide bond between Cys^{85} and Cys^{92} (Fig. 3B). Based on PDIA5 results, we argue that Cys^{85} and Cys^{92} of PDIA3 and for Cys^{291} and Cys^{297} of PDIA6 could also have an allosteric function. As discussed for PDIA5, this could influence the interaction with other partners or could bring the classical catalytic motif closer to the substrate and therefore control reduction, oxidation, and isomerization activities. In the case of PDIA6, this could also have an impact on the dimerization, which is strongly dependent on the conformational state [59,60].

5. Concluding remarks

In conclusion, based on Cysteine redoxome data and structural analyses, we propose the existence in several PDIAs of an additional non-catalytic thiol-disulfide motif containing Cys, distinct from those contained in TRX type motifs typical of PDIAs. The organization of the PDIA5 motif containing Cys^{451} and Cys^{456} intersects with that of a CX_4C thiol-disulfide center motif as found in human thioredoxin reductases (TR1 and 3) and in the GSSG reductase (GR) [61]. In TR and GR, the thiol-disulfide center is involved in the electrons shuttle from the enzyme to the substrate [61,62]. However, the CX_4C motif found in PDIA5 differs from those of TR and GR by the position of the disulfide bond. In TR and GR, the disulfide bond is formed between the 2 Cys of the CX_4C motif [61]. Instead in PDIA5, the modeled structure predicts a disulfide bond between Cys^{456}, the second Cys of the motif, and Cys^{465} located 8 residues apart, which rather refers to a CX_8C motif. Regarding Cys^{85} and Cys^{92} of PDIA3, they belong to a CX_6C motif similar to the one found in the a-type domain of the yeast protein disulfide isomerase Pdi1p. In Pdi1p, the 2 Cys form a disulfide bond whose presence is essential for the oxidase and isomerase activity of the catalytic Cys [47]. Presence of the CX_6C disulfide bond in PDIA3 could have a similar impact on the redox activity of the protein. As for PDIA6, Cys^{291} and Cys^{297} are organized into a CX_5C motif. This type of motif is found in the antimicrobial peptides limnonectin-1Fa and 1Fb, in which the two Cys form an intramolecular disulfide bond [48]. Chloroplast coupling factor 1 (CF1) also has a CX_5C motif of which the two Cys form a disulfide bond, the reduction of which increases ATPase activity [49]. Cys of the CX_5C motif in the atypical peroxiredoxin bacterioferritin co-migratory protein 1 (Bcp1) also form disulfide bonds and act as the conserved peroxidatic Cys (Cp) and resolving Cys (Cr) [50]. Thus, Cys of CX_5C motifs appear to be involved in disulfide bonds linked to protein activity. Consistent with this model, the Alphafold prediction of the CX_5C of PDIA6 also shows disulfide bond, suggesting a possible role of this motif in PDIA6 activity. As described in Table 1, several members of the PDI family exhibit CX_nC motifs distinct from those contained in TRX type motifs.

The hypothesis formulated in this paper calls for future experimental studies aimed at confirming the existence of these non-catalytic thiol-disulfide motifs and deciphering their exact role in the functions of PDIs should be considered. Primarily, since we cannot eliminate the possibility that modifications occurring at the mentioned residues are sulfinylations ($-SO_2H$) or sulfonylations ($-SO_3H$), this must be verified using

Table 1
CX_5C, CX_6C or CX_8C motifs found in PDIs.

PDI	Alternative names	Additional CX_nC motifs	Position of Cys	Domain localization
Protein disulfide-isomerase A3	Endoplasmic reticulum resident protein 57 (ERp57)/Endoplasmic reticulum resident protein 60 (ERp60)/Disulfide isomerase ER-60	CX_6C	Cys^{85}-Cys^{92}	1st catalytic TRX-like domain
Protein disulfide-isomerase A5	Protein disulfide isomerase-related protein (PDIR)	CX_8C	Cys^{85}-Cys^{94}	Non-catalytic TRX-like domain
		CX_8C	Cys^{456}-Cys^{465}	3rd catalytic TRX-like domain
Protein disulfide-isomerase A6	Endoplasmic reticulum protein 5 (ERp5)/Protein disulfide isomerase P5/Thioredoxin domain-containing protein 7	CX_5C	Cys^{291}-Cys^{297}	Non-catalytic TRX-like domain
Thioredoxin-related transmembrane protein 1 (TMX1)	Thioredoxin domain-containing protein 1/Transmembrane Trx-related protein.	CX_6C	Cys^{198}-Cys^{205}	1st catalytic TRX-like domain
Thioredoxin domain-containing protein 5 (TXNDC5)	Endoplasmic reticulum resident protein 46 (ERp46)/Thioredoxin-like protein p46.	CX_6C	Cys^{121}-Cys^{128}	1st catalytic TRX-like domain
		CX_6C	Cys^{247}-Cys^{254}	2nd catalytic TRX-like domain
		CX_6C	Cys^{381}-Cys^{388}	3rd catalytic TRX-like domain
DnaJ homolog subfamily C member 10 (DNAJC10)	Endoplasmic reticulum DNA J domain-containing protein 5 (ERdj5)/Macrothioredoxin (MTHr).	CX_6C	Cys^{186}-Cys^{193}	1st catalytic TRX-like domain
		CX_5C	Cys^{264}-Cys^{270}	Non-catalytic TRX-like domain
		CX_6C	Cys^{294}-Cys^{301}	Non-catalytic TRX-like domain
		CX_6C	Cys^{403}-Cys^{410}	Non-catalytic TRX-like domain
		CX_6C	Cys^{508}-Cys^{515}	2nd catalytic TRX-like domain
		CX_6C	Cys^{616}-Cys^{623}	3rd catalytic TRX-like domain
		CX_6C	Cys^{728}-Cys^{735}	4th catalytic TRX-like domain

specific labeling probes or antibodies combined with immunoblot or mass spectrometry approaches [63–65]. If these modifications are excluded, future research, performed in-silico and in-cell, should aim at exploring the type of redox modifications of Cys outside of the typical Trx-like domains of PDIAs, including the Cter $C^{456}X_8C^{465}$ motif of PDIA5, the $C^{85}X_6C^{92}$ motif of PDIA3 and the $C^{291}X_5C^{297}$ motif of PDIA6, and their role in PDIAs function. Confirmation of this activity will require site-directed mutagenesis-based studies to determine the redox-dependent interactome to identify potential substrates and the impact on substrate folding. High-speed atomic force microscopy (HS-AFM), which allows acquisition of successive AFM images during a period of times, grants exploration of how a purified protein can undergo dynamic conformational changes when a substrate is present in the environment. In the case of PDIA1, this has been useful to show that pretreatment of the purified protein with reducing or oxidizing agents leads to less or more compact conformations. For chaperone p97, HS-AFM has been successful to study the dynamic rotation of wild-type p97 and mutants when immersed in ATP containing buffers [66–69]. Therefore, HS-AFM would be an asset to explore how Cys mutations on PDIs or reducing vs oxidative environments shape the dynamics of PDIA3, PDIA5 and PDIA6 structures in the presence of newly identified substrates. Molecular dynamic simulations would also help deepen the redox-dependent conformational changes of PDIs. Ultimately, resolution of the structure of the full-length PDIA5 and PDIA6 or at minimum of the Cter region by cryo-electron microscopy in reducing and oxidative conditions should be considered to explore the proposition of novel non-catalytic thiol-disulfide motifs and understand the full scope of PDIs structure and function.

Author contributions

NZC analyzed the data. NZC and NG wrote the manuscript.

Declaration of competing interest

The authors declare that they have no known competing financial interests or personal relationships that could have appeared to influence the work reported in this paper.

Data availability

Data discussed in this hypothesis paper have been made publicly available as described in doi: 10.1126/scisignal.aaw4673.

Acknowledgments

The authors are grateful to Vikas Anathy, University of Vermont for critical reading of the manuscript. The present work was funded by grants from the Canadian Institutes of Health Research (CIHR) [MOP-137099, III-134054, and PJT-169021] to NG. NZC was recipient of graduate studentships from the Faculty of Medicine, the Faculty of postdoctoral and graduate studies, Université de Montréal, and the Fonds de recherche du Québec – Santé (FRQS). NZC and NG are members of the Quebec respiratory Health Research Network and of the Quebec COVID - Pandemic Network.

References

[1] C.E. Paulsen, K.S. Carroll, Cysteine-mediated redox signaling: chemistry, biology, and tools for discovery, Chem. Rev. 113 (7) (2013) 4633–4679.
[2] S.G. Rhee, I.S. Kil, Multiple functions and regulation of mammalian peroxiredoxins, Annu. Rev. Biochem. 86 (2017) 749–775.
[3] R. Radi, Oxygen radicals, nitric oxide, and peroxynitrite: redox pathways in molecular medicine, Proc. Natl. Acad. Sci. U. S. A. 115 (23) (2018) 5839–5848.
[4] O. Rudyk, P. Eaton, Biochemical methods for monitoring protein thiol redox states in biological systems, Redox Biol. 2 (2014) 803–813.
[5] J. Bolduc, K. Koruza, T. Luo, J. Malo Pueyo, T.N. Vo, D. Ezeriņa, J. Messens, Peroxiredoxins wear many hats: factors that fashion their peroxide sensing personalities, Redox Biol. 42 (2021), 101959.
[6] Y.M. Go, J.R. Roede, D.I. Walker, D.M. Duong, N.T. Seyfried, M. Orr, Y. Liang, K. D. Pennell, D.P. Jones, Selective targeting of the cysteine proteome by thioredoxin and glutathione redox systems, Mol. Cell. Proteomics : MCP 12 (11) (2013) 3285–3296.
[7] A.G. Irvine, A.K. Wallis, N. Sanghera, M.L. Rowe, L.W. Ruddock, M.J. Howard, R. A. Williamson, C.A. Blindauer, R.B. Freedman, Protein disulfide-isomerase interacts with a substrate protein at all stages along its folding pathway, PLoS One 9 (1) (2014), e82511.
[8] F. Mahmood, R. Xu, M.U.N. Awan, Y. Song, Q. Han, X. Xia, J. Zhang, PDIA3: structure, functions and its potential role in viral infections, Biomed. Pharmacother. 143 (2021), 112110.
[9] M. Okumura, H. Kadokura, K. Inaba, Structures and functions of protein disulfide isomerase family members involved in proteostasis in the endoplasmic reticulum, Free Radic. Biol. Med. 83 (2015) 314–322.
[10] A. Mishra, M.W.U. Kabir, M.T. Hoque, diSBPred: a machine learning based approach for disulfide bond prediction, Comput. Biol. Chem. 91 (2021), 107436.
[11] C. Wiedemann, A. Kumar, A. Lang, O. Ohlenschläger, Cysteines and disulfide bonds as structure-forming units: insights from different domains of life and the potential for characterization by NMR, Front. Chem. 8 (2020) 280.
[12] C. Patel, H. Saad, M. Shenkman, G.Z. Lederkremer, Oxidoreductases in glycoprotein glycosylation, folding, and ERAD, Cells 9 (9) (2020).
[13] Q. Wang, J. Guan, J. Wan, Z. Li, Disulfide based prodrugs for cancer therapy, RSC Adv. 10 (41) (2020) 24397–24409.
[14] L.W. Bergman, W.M. Kuehl, Co-translational modification of nascent immunoglobulin heavy and light chains, J. Supramol. Struct. 11 (1) (1979) 9–24.
[15] B. Xiong, V. Jha, J.K. Min, J. Cho, Protein disulfide isomerase in cardiovascular disease, Exp. Mol. Med. 52 (3) (2020) 390–399.
[16] E. Hahm, J. Li, K. Kim, S. Huh, S. Rogelj, J. Cho, Extracellular protein disulfide isomerase regulates ligand-binding activity of αMβ2 integrin and neutrophil recruitment during vascular inflammation, Blood 121 (19) (2013) 3789–3800, s1-3800.
[17] L.E. Powell, P.A. Foster, Protein disulphide isomerase inhibition as a potential cancer therapeutic strategy, Cancer Med. 10 (8) (2021) 2812–2825.
[18] J. Li, K. Kim, S.Y. Jeong, J. Chiu, B. Xiong, P.A. Petukhov, X. Dai, X. Li, R. K. Andrews, X. Du, P.J. Hogg, J. Cho, Platelet protein disulfide isomerase promotes glycoprotein ibα-mediated platelet-neutrophil interactions under thromboinflammatory conditions, Circulation 139 (10) (2019) 1300–1319.
[19] S. Vatolin, J.G. Phillips, B.K. Jha, S. Govindgari, J. Hu, D. Grabowski, Y. Parker, D. J. Lindner, F. Zhong, C.W. Distelhorst, M.R. Smith, C. Cotta, Y. Xu, S. Chilakala, R. R. Kuang, S. Tall, F.J. Reu, Novel protein disulfide isomerase inhibitor with anticancer activity in multiple myeloma, Cancer Res. 76 (11) (2016) 3340–3350.
[20] Y.S. Ma, S. Feng, L. Lin, H. Zhang, G.H. Wei, Y.S. Liu, X.L. Yang, R. Xin, Y. Shi, D. D. Zhang, C.Y. Jia, G.X. Lu, S.B. Xue, F. Yu, Z.W. Lv, J.B. Liu, G.R. Wang, D. Fu, Protein disulfide isomerase inhibits endoplasmic reticulum stress response and apoptosis via its oxidoreductase activity in colorectal cancer, Cell. Signal. 86 (2021), 110076.
[21] N. Chamberlain, B.R. Korwin-Mihavics, E.M. Nakada, S.R. Bruno, D.E. Heppner, D. G. Chapman, S.M. Hoffman, A. van der Vliet, B.T. Suratt, O. Dienz, J.F. Alcorn, V. Anathy, Lung epithelial protein disulfide isomerase A3 (PDIA3) plays an important role in influenza infection, inflammation, and airway mechanics, Redox Biol. 22 (2019), 101129.
[22] N. Rawarak, A. Suttitheptumrong, O. Reamtong, K. Boonnak, S.N. Pattanakitsakul, Protein disulfide isomerase inhibitor suppresses viral replication and production during antibody-dependent enhancement of Dengue virus infection in human monocytic cells, Viruses 11 (2) (2019).
[23] Z. Wang, Z. Zhou, Z.Y. Guo, C.W. Chi, Snapshot of the interaction between HIV envelope glycoprotein 120 and protein disulfide isomerase, Acta Biochim. Biophys. Sin. 42 (5) (2010) 358–362.
[24] J. Fu, J. Gao, Z. Liang, D. Yang, PDI-regulated disulfide bond formation in protein folding and biomolecular assembly, Molecules 26 (1) (2020).
[25] Z. Wang, H. Zhang, Q. Cheng, PDIA4: the basic characteristics, functions and its potential connection with cancer, Biomed. Pharmacother. 122 (2020), 109688.
[26] A.K. Wallis, A. Sidhu, L.J. Byrne, M.J. Howard, L.W. Ruddock, R.A. Williamson, R. B. Freedman, The ligand-binding b' domain of human protein disulphide-isomerase mediates homodimerization, Protein Sci. : A Pub. Protein Soc. 18 (12) (2009) 2569–2577.
[27] L.J. Byrne, A. Sidhu, A.K. Wallis, L.W. Ruddock, R.B. Freedman, M.J. Howard, R. A. Williamson, Mapping of the ligand-binding site on the b' domain of human PDI: interaction with peptide ligands and the x-linker region, Biochem. J. 423 (2) (2009) 209–217.
[28] S. Bastos-Aristizabal, G. Kozlov, K. Gehring, Structural insight into the dimerization of human protein disulfide isomerase, Protein Sci. : A Pub. Protein Soc. 23 (5) (2014) 618–626.
[29] P. Klappa, L.W. Ruddock, N.J. Darby, R.B. Freedman, The b' domain provides the principal peptide-binding site of protein disulfide isomerase but all domains contribute to binding of misfolded proteins, EMBO J. 17 (4) (1998) 927–935.
[30] L. Wang, X. Wang, C.C. Wang, Protein disulfide-isomerase, a folding catalyst and a redox-regulated chaperone, Free Radic. Biol. Med. 83 (2015) 305–313.
[31] G. Tian, S. Xiang, R. Noiva, W.J. Lennarz, H. Schindelin, The crystal structure of yeast protein disulfide isomerase suggests cooperativity between its active sites, Cell 124 (1) (2006) 61–73.

[32] R.B. Freedman, P. Klappa, L.W. Ruddock, Protein disulfide isomerases exploit synergy between catalytic and specific binding domains, EMBO Rep. 3 (2) (2002) 136–140.

[33] M.S. Kulp, E.M. Frickel, L. Ellgaard, J.S. Weissman, Domain architecture of protein-disulfide isomerase facilitates its dual role as an oxidase and an isomerase in Ero1p-mediated disulfide formation, J. Biol. Chem. 281 (2) (2006) 876–884.

[34] M. Matsusaki, S. Kanemura, M. Kinoshita, Y.-H. Lee, K. Inaba, M. Okumura, The protein disulfide isomerase family: from proteostasis to pathogenesis, Biochim. Biophys. Acta Gen. Subj. 1864 (2) (2020), 129338.

[35] J.J. Galligan, D.R. Petersen, The human protein disulfide isomerase gene family, Hum. Genom. 6 (1) (2012) 6.

[36] R. Vinaik, G. Kozlov, K. Gehring, Structure of the non-catalytic domain of the protein disulfide isomerase-related protein (PDIR) reveals function in protein binding, PLoS One 8 (4) (2013), e62021.

[37] T. Hayano, M. Kikuchi, Molecular cloning of the cDNA encoding a novel protein disulfide isomerase-related protein (PDIR), FEBS Lett. 372 (2–3) (1995) 210–214.

[38] G. Jansen, P. Määttänen, A.Y. Denisov, L. Scarffe, B. Schade, H. Balghi, K. Dejgaard, L.Y. Chen, W.J. Muller, K. Gehring, D.Y. Thomas, An interaction map of endoplasmic reticulum chaperones and foldases, Mol. Cell. Proteomics : MCP 11 (9) (2012) 710–723.

[39] T. Horibe, M. Gomi, D. Iguchi, H. Ito, Y. Kitamura, T. Masuoka, I. Tsujimoto, T. Kimura, M. Kikuchi, Different contributions of the three CXXC motifs of human protein-disulfide isomerase-related protein to isomerase activity and oxidative refolding, J. Biol. Chem. 279 (6) (2004) 4604–4611.

[40] E.L. Huttlin, L. Ting, R.J. Bruckner, F. Gebreab, M.P. Gygi, J. Szpyt, S. Tam, G. Zarraga, G. Colby, K. Baltier, R. Dong, V. Guarani, L.P. Vaites, A. Ordureau, R. Rad, B.K. Erickson, M. Wühr, J. Chick, B. Zhai, D. Kolippakkam, J. Mintseris, R. A. Obar, T. Harris, S. Artavanis-Tsakonas, M.E. Sowa, P. De Camilli, J.A. Paulo, J. W. Harper, S.P. Gygi, The BioPlex Network: a systematic exploration of the human interactome, Cell 162 (2) (2015) 425–440.

[41] E.L. Huttlin, R.J. Bruckner, J.A. Paulo, J.R. Cannon, L. Ting, K. Baltier, G. Colby, F. Gebreab, M.P. Gygi, H. Parzen, J. Szpyt, S. Tam, G. Zarraga, L. Pontano-Vaites, S. Swarup, A.E. White, D.K. Schweppe, R. Rad, B.K. Erickson, R.A. Obar, K. G. Guruharsha, K. Li, S. Artavanis-Tsakonas, S.P. Gygi, J.W. Harper, Architecture of the human interactome defines protein communities and disease networks, Nature 545 (7655) (2017) 505–509.

[42] C. Wan, B. Borgeson, S. Phanse, F. Tu, K. Drew, G. Clark, X. Xiong, O. Kagan, J. Kwan, A. Bezginov, K. Chessman, S. Pal, G. Cromar, O. Papoulas, Z. Ni, D. R. Boutz, S. Stoilova, P.C. Havugimana, X. Guo, R.H. Malty, M. Sarov, J. Greenblatt, M. Babu, W.B. Derry, E.R. Tillier, J.B. Wallingford, J. Parkinson, E. M. Marcotte, A. Emili, Panorama of ancient metazoan macromolecular complexes, Nature 525 (7569) (2015) 339–344.

[43] R. Oughtred, J. Rust, C. Chang, B.J. Breitkreutz, C. Stark, A. Willems, L. Boucher, G. Leung, N. Kolas, F. Zhang, S. Dolma, J. Coulombe-Huntington, A. Chatr-Aryamontri, K. Dolinski, M. Tyers, The BioGRID database: a comprehensive biomedical resource of curated protein, genetic, and chemical interactions, Protein Sci. : A Pub. Protein Soc. 30 (1) (2021) 187–200.

[44] R. Mnatsakanyan, S. Markoutsa, K. Walbrunn, A. Roos, S.H.L. Verhelst, R. P. Zahedi, Proteome-wide detection of S-nitrosylation targets and motifs using bioorthogonal cleavable-linker-based enrichment and switch technique, Nat. Commun. 10 (1) (2019) 2195.

[45] J. Ogura, L.W. Ruddock, N. Mano, Cysteine 343 in the substrate binding domain is the primary S-Nitrosylated site in protein disulfide isomerase, Free Radic. Biol. Med. 160 (2020) 103–110.

[46] X. Fu, B.T. Zhu, Human pancreas-specific protein disulfide isomerase homolog (PDIp) is redox-regulated through formation of an inter-subunit disulfide bond, Arch. Biochem. Biophys. 485 (1) (2009) 1–9.

[47] B. Wilkinson, R. Xiao, H.F. Gilbert, A structural disulfide of yeast protein-disulfide isomerase destabilizes the active site disulfide of the N-terminal thioredoxin domain, J. Biol. Chem. 280 (12) (2005) 11483–11487.

[48] Y. Wu, L. Wang, M. Zhou, C. Ma, X. Chen, B. Bai, T. Chen, C. Shaw, Limnonectins: a new class of antimicrobial peptides from the skin secretion of the Fujian large-headed frog (Limnonectes fujianensis), Biochimie 93 (6) (2011) 981–987.

[49] K.E. Hightower, R.E. McCarty, Proteolytic cleavage within a regulatory region of the gamma subunit of chloroplast coupling factor 1, Biochemistry 35 (15) (1996) 4846–4851.

[50] C. Sarcinelli, G. Fiorentino, E. Pizzo, S. Bartolucci, D. Limauro, Discovering antioxidant molecules in the archaea domain: peroxiredoxin Bcp1 from sulfolobus solfataricus protects H9c2 cardiomyoblasts from oxidative stress, 2016, Archaea (2016), 7424870.

[51] N. Zamorano Cuervo, A. Fortin, E. Caron, S. Chartier, N. Grandvaux, Pinpointing cysteine oxidation sites by high-resolution proteomics reveals a mechanism of redox-dependent inhibition of human STING, Sci. Signal. 14 (680) (2021).

[52] L. Song, F. Wang, Z. Dong, X. Hua, Q. Xia, Label-free quantitative phosphoproteomic profiling of cellular response induced by an insect cytokine paralytic peptide, J. Proteonomics 154 (2017) 49–58.

[53] M.H.D.R. Al Shweiki, S. Mönchgesang, P. Majovsky, D. Thieme, D. Trutschel, W. Hoehenwarter, Assessment of label-free quantification in discovery proteomics and impact of technological factors and natural variability of protein abundance, J. Proteome Res. 16 (4) (2017) 1410–1424.

[54] A. Keller, A.I. Nesvizhskii, E. Kolker, R. Aebersold, Empirical statistical model to estimate the accuracy of peptide identifications made by MS/MS and database search, Anal Chem. 74 (20) (2002) 5383–5392.

[55] A.I. Nesvizhskii, A. Keller, E. Kolker, R. Aebersold, A statistical model for identifying proteins by tandem mass spectrometry, Anal Chem. 75 (17) (2003) 4646–4658.

[56] J. Jumper, R. Evans, A. Pritzel, T. Green, M. Figurnov, O. Ronneberger, K. Tunyasuvunakool, R. Bates, A. Žídek, A. Potapenko, A. Bridgland, C. Meyer, S.A. A. Kohl, A.J. Ballard, A. Cowie, B. Romera-Paredes, S. Nikolov, R. Jain, J. Adler, T. Back, S. Petersen, D. Reiman, E. Clancy, M. Zielinski, M. Steinegger, M. Pacholska, T. Berghammer, S. Bodenstein, D. Silver, O. Vinyals, A.W. Senior, K. Kavukcuoglu, P. Kohli, D. Hassabis, Highly accurate protein structure prediction with AlphaFold, Nature 596 (7873) (2021) 583–589.

[57] M. Varadi, S. Anyango, M. Deshpande, S. Nair, C. Natassia, G. Yordanova, D. Yuan, O. Stroe, G. Wood, A. Laydon, A. Žídek, T. Green, K. Tunyasuvunakool, S. Petersen, J. Jumper, E. Clancy, R. Green, A. Vora, M. Lutfi, M. Figurnov, A. Cowie, N. Hobbs, P. Kohli, G. Kleywegt, E. Birney, D. Hassabis, S. Velankar, AlphaFold Protein Structure Database: massively expanding the structural coverage of protein-sequence space with high-accuracy models, Nucleic Acids Res. 50 (D1) (2021) D439–D444.

[58] A. Warnecke, T. Sandalova, A. Achour, R.A. Harris, PyTMs: a useful PyMOL plugin for modeling common post-translational modifications, BMC Bioinf. 15 (1) (2014) 370.

[59] M. Okumura, S. Kanemura, M. Matsusaki, M. Kinoshita, T. Saio, D. Ito, C. Hirayama, H. Kumeta, M. Watabe, Y. Amagai, Y.H. Lee, S. Akiyama, K. Inaba, A unique leucine-valine adhesive motif supports structure and function of protein disulfide isomerase P5 via dimerization, Structure 29 (12) (2021) 1357–1370, e6.

[60] M. Matsusaki, R. Okada, Y. Tanikawa, S. Kanemura, D. Ito, Y. Lin, M. Watabe, H. Yamaguchi, T. Saio, Y.H. Lee, K. Inaba, M. Okumura, Functional interplay between P5 and PDI/ERp72 to drive protein folding, Biology 10 (11) (2021).

[61] Q.A. Sun, L. Kirnarsky, S. Sherman, V.N. Gladyshev, Selenoprotein oxidoreductase with specificity for thioredoxin and glutathione systems, Proc. Natl. Acad. Sci. U. S. A. 98 (7) (2001) 3673–3678.

[62] M.A. Wouters, S.W. Fan, N.L. Haworth, Disulfides as redox switches: from molecular mechanisms to functional significance, Antioxidants Redox Signal. 12 (1) (2010) 53–91.

[63] M. Lo Conte, J. Lin, M.A. Wilson, K.S. Carroll, A chemical approach for the detection of protein sulfinylation, ACS Chem. Biol. 10 (8) (2015) 1825–1830.

[64] H.A. Woo, S.W. Kang, H.K. Kim, K.S. Yang, H.Z. Chae, S.G. Rhee, Reversible oxidation of the active site cysteine of peroxiredoxins to cysteine sulfinic acid. Immunoblot detection with antibodies specific for the hyperoxidized cysteine-containing sequence, J. Biol. Chem. 278 (48) (2003) 47361–47364.

[65] Y.H. Seo, K.S. Carroll, Profiling protein thiol oxidation in tumor cells using sulfenic acid-specific antibodies, Proc. Natl. Acad. Sci. U. S. A. 106 (38) (2009) 16163–16168.

[66] T. Uchihashi, R. Iino, T. Ando, H. Noji, High-speed atomic force microscopy reveals rotary catalysis of rotorless F_1-ATPase, Science 333 (6043) (2011) 755–758.

[67] T. Uchihashi, N. Kodera, T. Ando, Guide to video recording of structure dynamics and dynamic processes of proteins by high-speed atomic force microscopy, Nat. Protoc. 7 (6) (2012) 1193–1206.

[68] K. Noi, D. Yamamoto, S. Nishikori, K.-i. Arita-Morioka, T. Kato, T. Ando, T. Ogura, High-speed atomic force microscopic observation of ATP-dependent rotation of the AAA+ chaperone p97, Structure 21 (11) (2013) 1992–2002.

[69] M. Okumura, K. Noi, S. Kanemura, M. Kinoshita, T. Saio, Y. Inoue, T. Hikima, S. Akiyama, T. Ogura, K. Inaba, Dynamic assembly of protein disulfide isomerase in catalysis of oxidative folding, Nat. Chem. Biol. 15 (5) (2019) 499–509.